



Published in final edited form as:

Circulation. 2009 September 15; 120(11 Suppl): S230–S237. doi:10.1161/CIRCULATIONAHA.108.841155.

Novel Minicircle Vector for Gene Therapy in Murine Myocardial Infarction

Mei Huang, PhD¹, ZhiYing Chen, MD², Shijun Hu, PhD¹, Fangjun Jia, PhD¹, Zongjin Li, MD, PhD¹, Grant Hoyt, BS³, Robert C. Robbins, MD³, Mark A. Kay, MD, PhD², and Joseph C. Wu, MD, PhD^{1,4}

¹Department of Radiology, Stanford, CA 94306, USA

²Department of Pediatrics, Stanford, CA 94306, USA

³Department of Cardiothoracic Surgery, Stanford, CA 94306, USA

⁴Department of Medicine, Division of Cardiology, Stanford, CA 94306, USA

Abstract

Background—Conventional plasmids for gene therapy produce low-level and short-term gene expression. In this study, we develop a novel non-viral vector which robustly and persistently expresses the hypoxia inducible factor-1 alpha (HIF-1 α) therapeutic gene in the heart, leading to functional benefits following myocardial infarction (MI).

Methods and Results—We first created minicircles carrying double fusion (MC-DF) reporter gene consisting of firefly luciferase and enhanced green fluorescent protein (Fluc-eGFP) for noninvasive measurement of transfection efficiency. Mouse C2C12 myoblasts and normal FVB mice were used for *in vitro* and *in vivo* confirmation, respectively. Bioluminescence imaging (BLI) showed stable minicircle gene expression in the heart for >12 weeks and the activity level was 5.6 \pm 1.2 fold stronger than regular plasmid at day 4 (P <0.01). Next, we created minicircles carrying hypoxia inducible factor-1 alpha (MC-HIF-1 α) therapeutic gene for treatment of MI. Adult FVB mice underwent LAD ligation and were injected intramyocardially with (1) MC-HIF-1 α , (2) regular plasmid carrying HIF-1 α (PL-HIF-1 α) as positive control, and (3) PBS as negative control (n=10/group). Echocardiographic study showed a significantly greater improvement of left ventricular ejection fraction (LVEF) in the minicircle group (51.3% \pm 3.6%) compared to regular plasmid group (42.3% \pm 4.1%) and saline group (30.5% \pm 2.8%) at week 4 (P <0.05 for both). Histology demonstrated increased neoangiogenesis in both treatment groups. Finally, Western blot showed minicircles express >50% higher HIF-1 α level than regular plasmid.

Conclusion—Taken together, this is the first study to demonstrate that minicircles can significantly improve transfection efficiency, duration of transgene expression, and cardiac contractility. Given the serious drawbacks associated with most viral vectors, we believe this novel non-viral vector can be of great value for cardiac gene therapy protocols.

Keywords

minicircle; Φ C31 recombinase; molecular imaging; hypoxia inducible factor; ischemic heart disease

Correspondence: Joseph C. Wu, MD, PhD, Stanford University School of Medicine, Edwards Building R354, Stanford, CA 94305-5344, Ph: 650-736-2246, Fax: 650-736-0234, joewu@stanford.edu.

Statement of Responsibility: The authors had full access to and take full responsibility for the integrity of the data. All authors have read and accept the manuscript as written.

Disclosures. None.

INTRODUCTION

One of the most important objectives in gene therapy is the development of safe and efficient systems for gene transfer in eukaryotic cells. There are two strategies to provide target genes for gene transfer, viral and non-viral based systems¹. Although viral-based systems have shown high transfection efficiency *in vivo*, they suffer from serious disadvantages such as immunogenicity and inflammatory response². Nonviral gene delivery strategies are usually based on plasmid DNA carrying the gene of interest. Plasmid DNA is utilized in ~25% of all clinical gene therapy trials as of mid 2007³. Conventional plasmid vectors include a bacterial backbone and a transcription unit. However, these sequences may cause undesirable effects such as the production of antibodies against bacterial proteins expressed from cryptic upstream eukaryotic expression signals, changes in eukaryotic gene expression caused by the antibiotic resistance marker, and immune responses to CpG sequences⁴.

Compared to conventional plasmids, minicircles are supercoiled DNA molecules that are smaller and that lack a bacterial origin of replication and an antibiotic resistance gene⁵. Minicircles are obtained in *E. coli* by att site-specific recombination mediated by the bacteriophage Φ 31 integrase (Figure 1A). Minicircles may contain no more than an eukaryotic expression cassette and the attR fragment resulting from the attP/attB recombination event. Thus, they constitute a safe non-transmissible genetic material for nonviral gene therapy^{6, 7}.

Coronary artery disease (CAD) is the leading cause of morbidity and mortality in the Western world⁸. One of the most efficient approaches to treat patients with CAD is to deliver potent angiogenic factors to stimulate new vessel growth. HIF-1 α is known to control the expression of over 60 genes that affect cell survival and metabolism in adverse conditions, including vascular endothelial growth factor (VEGF), fibroblast growth factor (FGF), insulin-like growth factor (IGF), erythropoietin, nitric oxide synthase, among others⁹. With the use of various gene transfer techniques, it is now possible to modify cardiac cells to over-express beneficial proteins or inhibit pathologic proteins and achieve desired therapeutic effects. In this study, we have developed novel non-viral minicircles capable of transferring a reporter gene (Fluc-eGFP) and a therapeutic gene (HIF-1 α) with higher efficiency than regular plasmids both *in vitro* and *in vivo*. Our results suggest that the use of minicircles may offer a promising avenue for safe and efficacious non-viral based cardiac gene therapy in the future.

MATERIALS AND METHODS

Construction of minicircle plasmids

For the production of minicircle with ubiquitin promoter driving double fusion (MC-DF), firefly luciferase and enhanced green fluorescent protein (Fluc-eGFP) was amplified with FG-forward (5'-CCGAATTCATGAACCTTCTGCTGTCTTGGG) and FG-reverse (5'-AAAAGCGGCCGCTCATTCATTCATCAC) using pUbiquitin-Fluc-eGFP as a template (Figure 1B) (FG denotes Fluc/GFP). Amplification conditions are as follow: 2 min at 94°C for initial denaturation, then 30 cycles of 30 sec at 94°C for denaturation, 30 sec at 63.4°C for annealing, and 1 min at 68°C for extension, and then 10 min at 72°C for the final extension. All PCRs were carried out in MyCycler™ (Bio-Rad, CA, USA). For the production of minicircle with ubiquitin promoter driving HIF-1 α therapeutic gene (MC-HIF-1 α), the DNA fragment which contains the ubiquitin promoter, the HIF-1 α cDNA, and SV40 poly adenylation signal sequence was excised with EcoRI and XbaI from the pcDNA3.1-HIF-1 α , and then bluntly ligated between the attB and attP sites of the p2 ϕ C31

plasmid (Figure 1C). Note we used a mutant version of the HIF-1 α , which was created by site-specific mutation of P402 and P564 (P402A/P564G), rendering it less prone to hydroxylation and proteosomal degradation as previously described (a kind gift from Dr. Amato Giaccia, Department of Radiation Oncology)¹⁰.

Preparation and amplification of minicircle DNA

E. coli Top10 (Invitrogen) was transformed by parental plasmids. A single colony of the transformants was grown at 37°C overnight (OD₆₀₀ = 4.5–5.0). The 1 L of bacterial culture in the steady state was spun down in a centrifuge (rotor JA-14, J2-MC centrifuge, Beckman, Fullerton, CA, USA) at 1300g for 15 min at 20°C. The pellet was re-dissolved with 1 L of fresh LB broth (pH 7.0) containing 1% L-(+)-arabinose. The resuspended bacteria were incubated at 30°C with constant shaking at 225 rpm for 2 hr. Subsequently, 1 L of fresh LB broth (pH 8.0) containing 1% L-(+)-arabinose was added to the culture and the bacteria were cultivated for additional 2 hr at 37°C for the activation of the restriction enzyme I-SceI, which cuts and linearizes the bacterial backbone plasmids and subject them for degradation (see Figure 1). Super-coiled minicircle DNA was isolated from the culture, using plasmid purification kits from the Qiagen (Valencia, CA). The contaminated endotoxin in the DNA preparation was removed by the AffinityPak Detoxi-Gel (Pierce, Rockford, IL).

Cell culture and transfection

Mouse C2C12 myoblast cells were cultured in DMEM containing 10% fetal bovine serum (FBS). All cells were maintained in a 5% CO₂ incubator. For the transfection, cells were seeded at a density of 5×10^5 cells/well in the six-well flat-bottomed micro-assay plates (Falcon Co., Becton Dickenson, Franklin Lakes, NJ) 24 hr before the transfection. At 70–80% confluency, cells were transfected with 4 μ g of plasmids carrying the double fusion reporter gene (PL-DF) or equimolar 2 μ g of minicircles carrying the DF reporter gene (MC-DF) and incubated for an additional 48 hr. Lipofectamine 2000 (Invitrogen) was used for the transfection according to the manufacturer's protocol.

Noninvasive bioluminescence imaging (BLI) to assess duration of reporter gene expression

To compare the duration of gene expression *in vivo*, 25 μ g of PL-DF and 12.5 μ g of MC-DF were injected into normal mouse hearts following aseptic open thoracotomy (n=5 per group). BLI was performed with the Xenogen In Vivo Imaging System (Alameda, CA) on days 0, 1, 4, 7, 21, 42, 60, and 90 by an investigator blinded to study conditions (SH). After intraperitoneal injection of the reporter probe D-luciferin (150 mg/kg body weight), animals were imaged. The same mice were scanned repetitively according to the specific study design. BLI signals were quantified in maximum photons per second per centimeter squared per steradian (p/s/cm²/sr) as described¹¹. Briefly, after anesthetic induction with 2% isoflurane, reporter probe D-luciferin (Promega) was injected into the peritoneal cavity. After waiting for 10 min to allow D-luciferin biodistribution, the animals were placed in a light-tight chamber and baseline gray-scale body-surface images were taken. Photons emitted from Fluc/D-luciferin photochemical reaction within the animal were acquired repetitively (1–10 min acquisition time per image, 5–15 images per animal) until peak value was confirmed. We then averaged the 3 images with the highest p/sec/cm²/sr values and used that to represent the Fluc transgene expression for that mouse on that particular day.

Animal surgery to induce myocardial infarction (MI)

Ligation of the mid left anterior descending (LAD) artery was performed in adult female FVB mice (Charles River Laboratories, Wilmington, MA) by a single experienced microsurgeon (GH). MI was confirmed by myocardial blanching and EKG changes. After

waiting for 10 min, animals were then injected intramyocardially with 12.5 µg of minicircles carrying HIF-1α (MC-HIF-1α), or equimolar 25 µg of regular plasmids carrying HIF-1α (PL-HIF-1α) as positive control, or PBS as negative control (n=10 per group). Injections were made near the peri-infarct region at 3 different sites with a total volume of 25 µl using a 31-gauge Hamilton syringe. Study protocols were approved by the Stanford Animal Research Committee.

Analysis of left ventricular function with echocardiogram

Echocardiography was performed before (day -7) and after (week 2, week 4, and week 8) the LAD ligation. The Siemens-Acuson Sequoia C512 system equipped with a multi-frequency (8–14 MHz) 15L8 transducer was used by an investigator (ZL) blinded to group designation. Left ventricular (LV) end diastolic (EDV) and end-systole volume (ESV) were calculated by the bullet method as follows: $EDV = 0.85 \times CSA(d) \times L(d)$, $ESV = 0.85 \times CSA(s) \times L(s)$, where $CSA(d)$ and (s) are endocardial cross sectional areas in end-diastole and end-systole, respectively, obtained from short-axis view at the level of the papillary muscles and $L(d)$ and $L(s)$ are the LV length (apex to mid-mitral annulus plane) in end-diastole and end-systole, respectively, obtained from the parasternal long-axis view. The left ventricular ejection fraction was calculated as: $LVEF\% = (EDV - ESV) \times 100/EDV$ as described¹².

Western blot of mouse hearts to assess HIF-1α levels

In order to determine the extent of HIF-1α activation following different experimental conditions, we randomized mice to sham surgery (open thoracotomy only), ischemia-reperfusion for 30 min, and LAD infarction (n=3 per group). Hearts from these animals were assayed for HIF-1α levels using Western blots on week 1, week 2 and week 3. After cutting the infarction part of the left ventricle under 10X microscope, we isolated tissue protein by Ripa buffer (Sigma). Protein concentration of lysis supernatant was determined by the DC protein assay (Bio-Rad protocol). Whole tissue extracts (25 µg) in equal volume of 2x loading buffer were run onto 10% Tris-glycine SDS-PAGE gels and transferred to Hybond ECL membrane (Amersham). Protein blots were analyzed with rat anti-mouse HIF-1α (1/500 dilution, Novus) followed by sheep anti-rat IgG whole antibody-HRP secondary (1/3000 dilution, Amersham) and developed using ECL assay (Amersham).

Histological examination

Explanted hearts from study and control groups were embedded into OCT compound (Miles Scientific, Elkhart, IN). Frozen sections (5 µm thick) were processed for immunostaining. To quantify the left ventricular infarct size, trichrome staining was done in PBS, plasmid, and minicircle-treated hearts (n=4 per group). For each heart, eight to ten sections from apex to base (1.2 mm apart) were analyzed. Images were taken for each section to calculate the fibrotic and non-fibrotic areas as well as ventricular and septal wall thickness. Scarring was determined as fibrotic area/(fibrotic + nonfibrotic area) as previously described¹³. The NIH Image J software was used to quantify the infarct zones. To detect microvascular density (MVD) in the peri-infarct area, a rat anti-CD31 (BD Pharmingen) was used. The number of capillary vessels was counted by a blinded investigator (FJ) in ten randomly selected areas using the picture under a fluorescent microscope (x100 magnification). A typical green color vessel was selected as sample after opening one picture randomly by Image J software. The process was repeated 10 times in different per-infarct areas to calculate vessels numbers at 1 mm² scale. Additional samples were used to examine the infarction size by H&E staining.

Comparison of viral vs. non-viral vectors

In order to determine the duration of gene expression and the effects of immunologic response on viral vs. non-viral vectors, adult immunocompetent female FVB mice were injected with recombinant adeno-associated virus serotype 9 carrying CMV promoter driving firefly luciferase (AAV-Fluc at 1×10^9 pfu; gift from Roger Hajjar, Mount Sinai School of Medicine), 12.5 μ g of MC-DF, or 25 μ g of PL-Fluc in the right leg. Animals were imaged on days 1, 3, 7, 14, 21, and 28 using the Xenogen IVIS system. Afterwards, the same animals were injected with equal dosage of the same vectors into the left legs and imaging was performed at the same time points.

Statistical analysis

ANOVA and repeated measures ANOVA with post-hoc testing as well as the two-tailed Student's *t*-test were used. Differences were considered significant at *P*-values of ≤ 0.05 .

RESULTS

Intramolecular recombination splits parental plasmid into minicircle and bacterial backbone

Minicircles are the product of site-specific intramolecular recombination between the attB and attP sites driven by bacteriophage Φ C31 integrase. After isolation from the bacterial backbone (Figure 1A), the minicircles now lack both an origin of replication (cannot self-replicate) and an antibiotic selection marker (cannot confer resistance to other microorganisms), and carry only short bacterial sequences (greatly limiting immune responses against CpG sequences in the bacterial backbone). In this study, we first constructed MC-DF that allowed us to determine the transfection efficiency (in C2C12 cells) and duration of transgene expression (in living animals). The Fluc-eGFP cDNA was successfully cloned by PCR and ligated into the parental plasmid p2 Φ c31.UB-DF (Figure 1B). We next constructed MC-HIF-1 α that allowed us to assess the therapeutic efficacy of MC vs. PL-based gene therapy approaches (Figure 1C). The HIF-1 α gene was successfully ligated into the parental plasmid p2 Φ c31.UB-HIF-1 α . We used the ubiquitin promoter (UB) for both parental plasmids because it has been shown to drive high levels of transgene expression with minimal gene silencing¹⁴. By addition of arabinose at 32°C, the phage Φ C31 integrase performs a site-specific intramolecular recombination of sequences between attB and attP recognition sites, splitting p2 Φ C31 parental plasmid into two super-coiled circular DNAs: the minicircle with its transgene of interest and the remaining DNA with a “junk” bacterial backbone. To physically separate the two end products, we then adjust the pH and temperature to pH 8.0 and 37°C, respectively. The bacterial backbone plasmid is linearized by the induced I-SceI and degraded by bacterial exonucleases (Figure 1B–1C). As a consequence, only the minicircle containing the transgene of interest in our study (DF and HIF-1 α) remained intact as an episome formation in the bacterial cytosol, which can then be isolated for subsequent usage.

Evaluation of novel minicircles vs. regular plasmids in cell line

To assess the transfection efficiency, equimolar amounts of MC-DF and PL-DF were used to transfect mouse C2C12 cells. Fluc was evaluated by BLI (Figure 2A) and eGFP evaluated by flow cytometry (Figure 2B). MC-DF showed 5.5 ± 1.7 -fold (at 12 hr) and 8.1 ± 2.8 -fold (at 48 hr) higher Fluc expression compared to PL-DF. Since the DF is fusion construct whereby the two reporter genes are linked by a 5-amino acid linker (GSHGD), MC-DF also showed earlier onset of eGFP activity by 12 hrs (8.16 ± 0.04 vs. $0.23 \pm 0.03\%$, $P < 0.01$) as expected. Overall, these data demonstrate minicircles can mediate faster and higher transgene expression *in vitro* than regular plasmids.

Comparison of novel minicircle vs. regular plasmids in living animals

To determine expression level *in vivo*, we next injected MC-DF and PL-DF into normal mouse hearts and followed their gene expression from day 0 to day 90 using BLI (Figure 3A). Quantitative analyses of Fluc activities for both groups are shown in Figure 3B. Overall, mice injected with MC-DF had significantly higher Fluc activity compared to mice injected with PL-DF at day 1 ($2.6 \times 10^6 \pm 7.9 \times 10^3$ vs. $1.4 \times 10^4 \pm 1.3 \times 10^3$, $P < 0.001$), day 7 ($3.2 \times 10^6 \pm 1.5 \times 10^4$ vs. $6.79 \times 10^5 \pm 4.2 \times 10^3$, $P < 0.0001$), day 14 ($2.8 \times 10^6 \pm 2.6 \times 10^4$ vs. $9.7 \times 10^5 \pm 8.6 \times 10^3$, $P < 0.0001$), day 28 ($8.9 \times 10^5 \pm 4.1 \times 10^3$ vs. $1.6 \times 10^5 \pm 3.9 \times 10^3$, $P < 0.001$), day 42 ($7.4 \times 10^5 \pm 8.7 \times 10^3$ vs. $1.3 \times 10^5 \pm 2.9 \times 10^3$, $P < 0.0001$), day 60 ($6.5 \times 10^5 \pm 5.7 \times 10^3$ vs. $1.3 \times 10^5 \pm 3.8 \times 10^3$, $P < 0.0001$), and day 90 ($4.4 \times 10^5 \pm 2.1 \times 10^3$ vs. $1.45 \times 10^4 \pm 3.1 \times 10^2$ p/s/cm²/sr, $P < 0.0001$). Overall, these data demonstrate minicircles can mediate stronger and longer transgene expression *in vivo* than regular plasmids.

Injection of minicircles carrying HIF-1 α improved cardiac function following MI

To examine whether using MC-HIF-1 α can also improve cardiac function following myocardial infarction, echocardiography was performed before (day -7) and after (week 2, week 4, and week 8) the LAD ligation. At day -7, the LVEF was comparable in all three groups (Figure 4). Following LAD ligation, the minicircle group had significantly higher ejection fraction compared to the PBS control group at both week 4 and week 8 ($P < 0.01$ for both). The regular plasmid group had significantly higher ejection fraction compared to the PBS group at week 4 (plasmid: $42.2 \pm 6.7\%$ vs. PBS: $35.1 \pm 5.5\%$, $P = 0.004$). However, this beneficial effect was no longer present by week 8 ($42.8 \pm 6.0\%$ vs. $37.8 \pm 3.4\%$; $P = 0.38$). This is likely due to the short-term transgene expression of regular plasmids (<4 weeks) as shown by our imaging results (Figure 3A).

Ex vivo histological validation of *in vivo* imaging data

After imaging, all animals were sacrificed and hearts explanted. H&E staining showed thicker heart wall size for the minicircle group compared to regular plasmid group and saline group at week 4, confirming the positive functional imaging data seen in echocardiography (Figure 5A). Minicircle treatment significantly decreased left ventricular scarring compared to plasmids and PBS control ($12.85 \pm 1.32\%$ vs. $21.5 \pm 3.51\%$ vs. $31.2 \pm 3.58\%$; $P = 0.045$ MC vs PL; $P = 0.001$ MC vs. PBS). Immunohistochemistry of the peri-infarct region by CD31 staining also showed increased neovascularization in the minicircle (389 ± 73.1) compared to the regular plasmid (251 ± 21.5) and PBS (138 ± 9.6 vessels/mm²) groups ($P < 0.05$ for both) (Figure 5B). To further confirm the *in vivo* functional imaging data, we assayed for HIF-1 α protein expression of explanted hearts at day 14. Quantitative analysis of the Western blot indicates that HIF-1 α proteins were significantly higher in the minicircle-treated hearts compared to regular plasmids and PBS-treated hearts (Figure 5C–D). Finally, we also investigated HIF-1 α expression levels in different ischemia conditions as well as in different time point after LAD ligation. Western blot data show that endogenous HIF-1 α is most robust following LAD ligation compared to ischemia-reperfusion and sham surgery, suggesting that activation of endogenous HIF-1 α expression level is directly related to the size of MI (Figure 5E). With co-administration of MC-HIF-1 α , highest levels of HIF-1 α are detected at week 1. The levels of MC-treated HIF-1 α decreases at subsequent week 2 and week 3, similar to the *in vivo* imaging pattern that was observed for Fluc transgene expression in Figure 3A.

Comparison of viral vs. non-viral vectors in FVB mice

Adenoviral vectors carrying either VEGF or FGF have been used for several cardiac gene therapy trials¹⁵. However, our group has previously shown that repeated injection of adenovirus induces a significant host cellular and humoral immune response¹⁶. Recently,

AAV has generated significant interest as a safer and more effective vehicle for cardiac gene transfer. Indeed, AAV carrying sarcoplasmic reticulum calcium ATPase (SERCA2a) has been used for treatment of patients with heart failure delivering¹⁷. Here we investigated the duration of gene expression after repeated intramuscular transplantation of AAV vs. minicircle and regular plasmid into immunocompetent adult female FVB mice (n=5 per group). Figure 6 shows that AAV-mediated Fluc expression was significantly higher compared to MC and PL after first injection as expected. At day 7, the activities were $1.42 \times 10^7 \pm 8.65 \times 10^5$ vs. $7.46 \times 10^6 \pm 5.52 \times 10^5$ vs. $2.85 \times 10^5 \pm 9.46 \times 10^4$ p/s/cm²/sr for each group, respectively ($P < 0.05$ AAV vs. MC and $P < 0.001$ AAV vs. PL). At day 28, the activities were $2.31 \times 10^6 \pm 6.3 \times 10^5$ vs. $3.34 \times 10^5 \pm 7.25 \times 10^4$ vs. $1.88 \times 10^4 \pm 3.51 \times 10^4$ p/s/cm²/sr, respectively ($P < 0.05$ AAV vs. MC and $P < 0.001$ AAV vs. PL). However, repeat administration of AAV in the contralateral leg at 4 weeks after primary injection resulted in no AAV-mediated signal expression. At day 28, the BLI signals for MC were comparable between first and second injection ($3.34 \times 10^5 \pm 7.25 \times 10^4$ vs. $2.15 \times 10^5 \pm 3.83 \times 10^4$; $P = \text{NS}$) whereas the BLI signals for AAV were significantly reduced ($2.31 \times 10^6 \pm 6.31 \times 10^5$ vs. $1.12 \times 10^4 \pm 6.46 \times 10^3$ p/s/cm²/sr; $P < 0.0001$). Taken together, these data suggest that AAV is capable of triggering both cellular and humoral immune response, which are consistent with two previous reports of dose-dependent generation of CD8⁺ T-cell responses to AAV capsid proteins in humans trials for treatment of hemophilia¹⁸ and type 1 hypertriglyceridemia deficiency¹⁹.

DISCUSSION

Although most phase 1 clinical trials in patients with myocardial ischemia provided encouraging results, more recent phase 2 randomized trials (AGENT, VIVA, and KAT) yielded inconsistent or modest benefits at best²⁰. These inconsistencies have been attributed to the lack of ideal vectors, inability to monitor gene transfer *in vivo*, and the unclear role of single therapeutic gene such as VEGF for inducing neovascularization. In this paper, we addressed these three issues by using a novel non-viral vector carrying a more robust therapeutic gene and validating the results with molecular imaging technology. The major findings are the following: (1) Minicircles can be easily isolated from the parental plasmid in *E. coli* culturing medium. In our study, we used the I-sceI site, a Φ c31 recombinase temperature sensitive recognition and cutting site to obtain large amounts of purified minicircles. (2) Minicircles show earlier onset and more robust transgene expression than conventional plasmids both *in vitro* and *in vivo*. In particular, flow cytometry data showed significant eGFP positivity by 12 hr compared to normal plasmids. BLI shows that MC-DF injected into murine hearts lasted >90 days, much longer than the 28 days seen in regular plasmids. (3) Direct injections of MC-HIF-1 α can improve ventricular function and enhance neoangiogenesis in a mouse model of myocardial infarction for 8 weeks, compared to 4 weeks for regular plasmids. (4) Lastly, repeated injections of MC have comparable transgene activities. In contrast, repeated injections of AAV lead to significant reduction of transgene expression due to host cellular and humoral immune response.

Non-viral vectors have many advantages over viral systems: a better safety profile, the absence of theoretical size limitation for the expression cassette, and possibly simpler clinical translation due to easier good manufacturing practices (GMP). On the other hand, concerns have been raised regarding (1) the lack of robust transfection efficiency and (2) the immunostimulatory prokaryotic CpG motives in the bacterial backbone. To resolve these issues, we designed the novel non-viral minicircle plasmids which exhibited up to eight-fold higher gene expression than the regular plasmid *in vitro* as well significantly longer transgene expression *in vivo*. This drastic improvement is due to the removal of unnecessary plasmid sequences, which could affect the gene expression, and the smaller size of the minicircles which might confer better extracellular and intracellular bioavailability and thus

improved gene delivery properties^{21, 22}. In particular, the bacterial backbone sequences are often abundant with CpG islands, which can lead to transcriptional gene silence *in vivo*, and is one of the major reasons why regular plasmids are notoriously ineffective for long-term expression²³.

The HIF-1 complex is known to control the expression of over 60 genes that affect cell survival and metabolism in adverse conditions⁹. As an upstream transcriptional factor, HIF-1 α is involved in activation of several pathways²⁴. Overexpression of HIF-1 α has critical functional consequences, including an improvement in neoangiogenesis due to upregulation of VEGF, FGF, and eNOS^{25, 26}. Importantly, recent evidence suggests that the expression of a single angiogenic factor such as VEGF alone may *not* be sufficient for the functional revascularization of ischemic tissues²⁷. Thus, newer approaches based on upregulation of the master regulator HIF-1 α may be a more potent choice. In this study, we selected HIF-1 α as a therapy target gene, which resulted in significant functional improvements after delivery into the infarcted hearts. Immunohistological results demonstrated that higher HIF-1 α expression led to formation of more small vessels which in turn improved cardiac function.

In summary, minicircles are novel non-viral vectors that lack an origin of replication and an antibiotic selection marker, and carry only short bacterial sequences. Our results suggest that using minicircles to deliver HIF-1 α may represent a potentially new therapeutic target in the field of cardiovascular gene therapy.

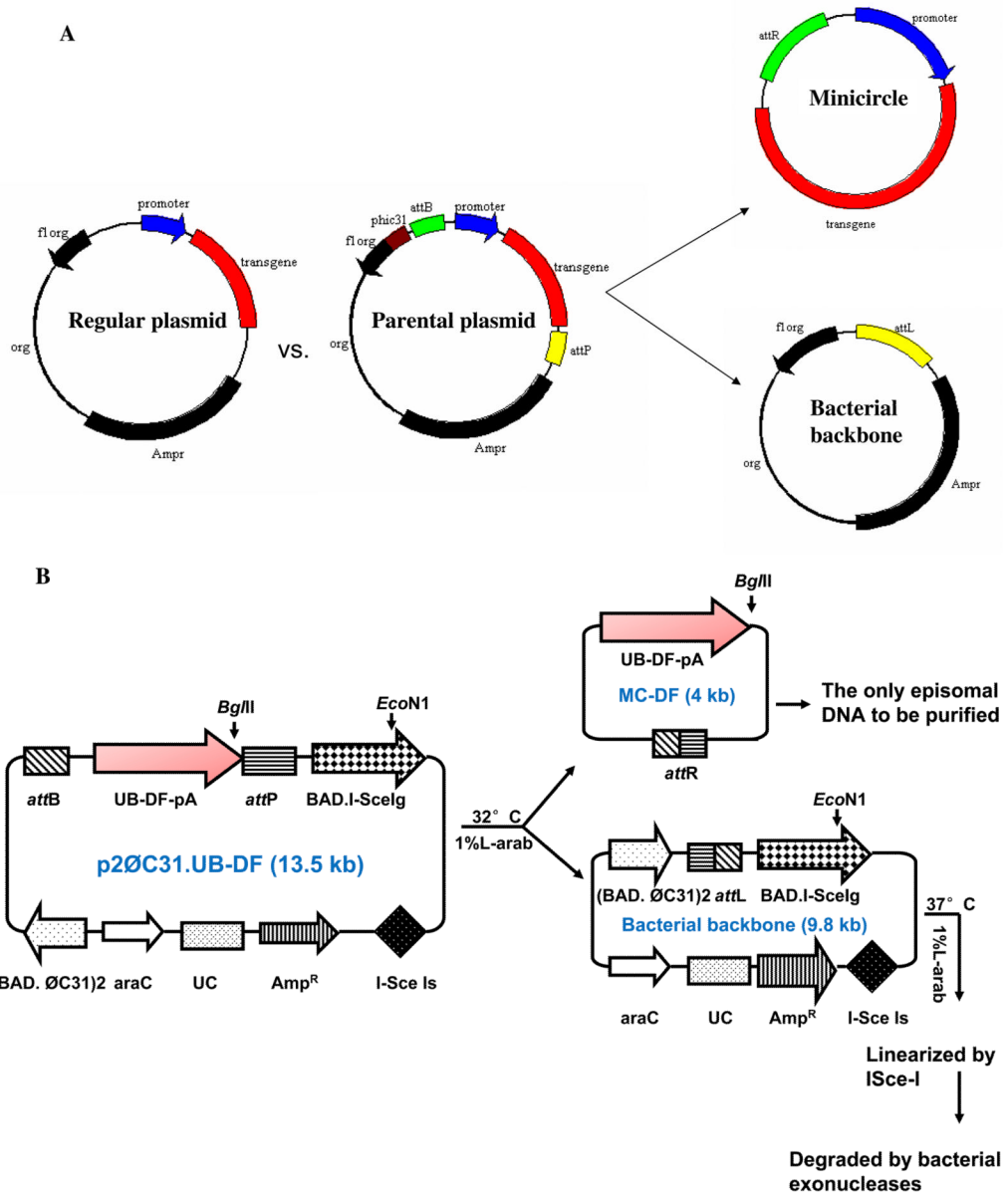
Acknowledgments

Funding Sources. This work was supported in part by grants from the NIH HL089027 (JCW), Baxter Faculty Scholar Award (JCW), and AHA Postdoctoral Fellowship (MH).

References

1. Lyon AR, Sato M, Hajjar RJ, Samulski RJ, Harding SE. Gene therapy: targeting the myocardium. *Heart*. 2008; 94:89–99. [PubMed: 18083952]
2. Marshall E. Gene therapy death prompts review of adenovirus vector. *Science*. 1999; 286:2244–2245. [PubMed: 10636774]
3. Edelstein ML, Abedi MR, Wixon J. Gene therapy clinical trials worldwide to 2007--an update. *The Journal of Gene Medicine*. 2007; 9:833–842. [PubMed: 17721874]
4. Jechlinger W. Optimization and delivery of plasmid DNA for vaccination. *Expert Review of Vaccines*. 2006; 5:803–825. [PubMed: 17184219]
5. Jechlinger W, Azimpour Tabrizi C, Lubitz W, Mayrhofer P. Minicircle DNA immobilized in bacterial ghosts: *in vivo* production of safe non-viral DNA delivery vehicles. *Journal of Molecular Microbiology and Biotechnology*. 2004; 8:222–231. [PubMed: 16179799]
6. Chen ZY, He CY, Meuse L, Kay MA. Silencing of episomal transgene expression by plasmid bacterial DNA elements *in vivo*. *Gene Therapy*. 2004; 11:856–864. [PubMed: 15029228]
7. Chen Z-Y, He C-Y, Kay MA. Improved production and purification of minicircle DNA vector free of plasmid bacterial sequences and capable of persistent transgene expression *in vivo*. *Human Gene Therapy*. 2005; 16:126–131. [PubMed: 15703495]
8. Rosamond W, Flegal K, Furie K, Go A, Greenlund K, Haase N, Hailpern SM, Ho M, Howard V, Kissela B, Kittner S, Lloyd-Jones D, McDermott M, Meigs J, Moy C, Nichol G, O'Donnell C, Roger V, Sorlie P, Steinberger J, Thom T, Wilson M, Hong Y. Heart disease and stroke statistics--2008 update: a report from the American Heart Association Statistics Committee and Stroke Statistics Subcommittee. *Circulation*. 2008; 117:e25–146. [PubMed: 18086926]
9. Yla-Herttuala S, Alitalo K. Gene transfer as a tool to induce therapeutic vascular growth. *Nature Medicine*. Jun.2003 9:694–701.

10. Yun Z, Lin Q, Giaccia AJ. Adaptive myogenesis under hypoxia. *Molecular and Cellular Biology*. Apr.2005 25:3040–3055. [PubMed: 15798192]
11. Cao F, Lin S, Xie X, Ray P, Patel M, Zhang X, Drukker M, Dylla SJ, Connolly AJ, Chen X, Weissman IL, Gambhir SS, Wu JC. In vivo visualization of embryonic stem cell survival, proliferation, and migration after cardiac delivery. *Circulation*. 2006; 113:1005–1014. [PubMed: 16476845]
12. Nemoto S, DeFreitas G, Mann DL, Carabello BA. Effects of changes in left ventricular contractility on indexes of contractility in mice. *American Journal of Physiology*. Dec.2002 283:H2504–2510. [PubMed: 12427596]
13. Engel FB, Hsieh PCH, Lee RT, Keating MT. FGF1/p38 MAP kinase inhibitor therapy induces cardiomyocyte mitosis, reduces scarring, and rescues function after myocardial infarction. *Proceedings of the National Academy of Sciences of the United States of America*. 2006; 103:15546–15551. [PubMed: 17032753]
14. Gill DR, Smyth SE, Goddard CA, Pringle IA, Higgins CF, Colledge WH, Hyde SC. Increased persistence of lung gene expression using plasmids containing the ubiquitin C or elongation factor 1alpha promoter. *Gene Therapy*. 2001; 8:1539–1546. [PubMed: 11704814]
15. Hiona A, Wu JC. Noninvasive radionuclide imaging of cardiac gene therapy: progress and potential. *Nature Clinical Practice Cardiovascular Medicine*. 2008; 5(Suppl 2):S87–95.
16. Wu JC, Chen IY, Wang Y, Tseng JR, Chhabra A, Salek M, Min J-J, Fishbein MC, Crystal R, Gambhir SS. Molecular imaging of the kinetics of vascular endothelial growth factor gene expression in ischemic myocardium. *Circulation*. 2004; 110:685–691. [PubMed: 15302807]
17. Hajjar RJ, Zsebo K, Deckelbaum L, Thompson C, Rudy J, Yaroshinsky A, Ly H, Kawase Y, Wagner K, Borow K, Jaski B, London B, Greenberg B, Pauly DF, Patten R, Starling R, Mancini D, Jessup M. Design of a phase 1/2 trial of intracoronary administration of AAV1/SERCA2a in patients with heart failure. *Journal of Cardiac Failure*. 2008; 14:355–367. [PubMed: 18514926]
18. Manno CS, Pierce GF, Arruda VR, Glader B, Ragni M, Rasko JJ, Rasko J, Ozelo MC, Hoots K, Blatt P, Konkle B, Dake M, Kaye R, Razavi M, Zajko A, Zehnder J, Rustagi PK, Nakai H, Chew A, Leonard D, Wright JF, Lessard RR, Sommer M Jr, Tigges M, Sabatino D, Luk A, Jiang H, Mingozzi F, Couto L, Ertl HC, High KA, Kay MA. Successful transduction of liver in hemophilia by AAV-Factor IX and limitations imposed by the host immune response. *Nature Medicine*. 2006; 12:342–347.
19. Mingozzi F, High KA. Immune responses to AAV in clinical trials. *Current Gene Therapy*. 2007; 7:316–324. [PubMed: 17979678]
20. Wu JC, Yla-Herttuala S. Human gene therapy and imaging: cardiology. *Eur J Nucl Med Mol Imaging*. Dec; 2005 32(Suppl 2):S346–357. [PubMed: 16096829]
21. Darquet AM, Cameron B, Wils P, Scherman D, Crouzet J. A new DNA vehicle for nonviral gene delivery: supercoiled minicircle. *Gene Therapy*. 1997; 4:1341–1349. [PubMed: 9472558]
22. Darquet AM, Rangara R, Kreiss P, Schwartz B, Naimi S, Delaère P, Crouzet J, Scherman D. Minicircle: an improved DNA molecule for in vitro and in vivo gene transfer. *Gene Therapy*. 1999; 6:209–218. [PubMed: 10435105]
23. Chen Z-Y, Riu E, He C-Y, Xu H, Kay MA. Silencing of episomal transgene expression in liver by plasmid bacterial backbone DNA is independent of CpG methylation. *Molecular Therapy*. 2008; 16:548–556. [PubMed: 18253155]
24. Giaccia A, Siim BG, Johnson RS. HIF-1 as a target for drug development. *Nature reviews. Drug Discovery*. 2003; 2:803–811.
25. Kleiman NS, Patel NC, Allen KB, Simons M, Ylä-Herttuala S, Griffin E, Dzau VJ. Evolving revascularization approaches for myocardial ischemia. *The American Journal of Cardiology*. 2003; 92:9–17N.
26. Huang M, Chan DA, Jia F, Xie X, Li Z, Hoyt G, Robbins RC, Chen X, Giaccia AJ, Wu JC. Short hairpin RNA interference therapy for ischemic heart disease. *Circulation*. 2008; 118:S226–233. [PubMed: 18824759]
27. Pislaru S, Janssens SP, Gersh BJ, Simari RD. Defining gene transfer before expecting gene therapy: putting the horse before the cart. *Circulation*. 2002; 106:631–636. [PubMed: 12147548]



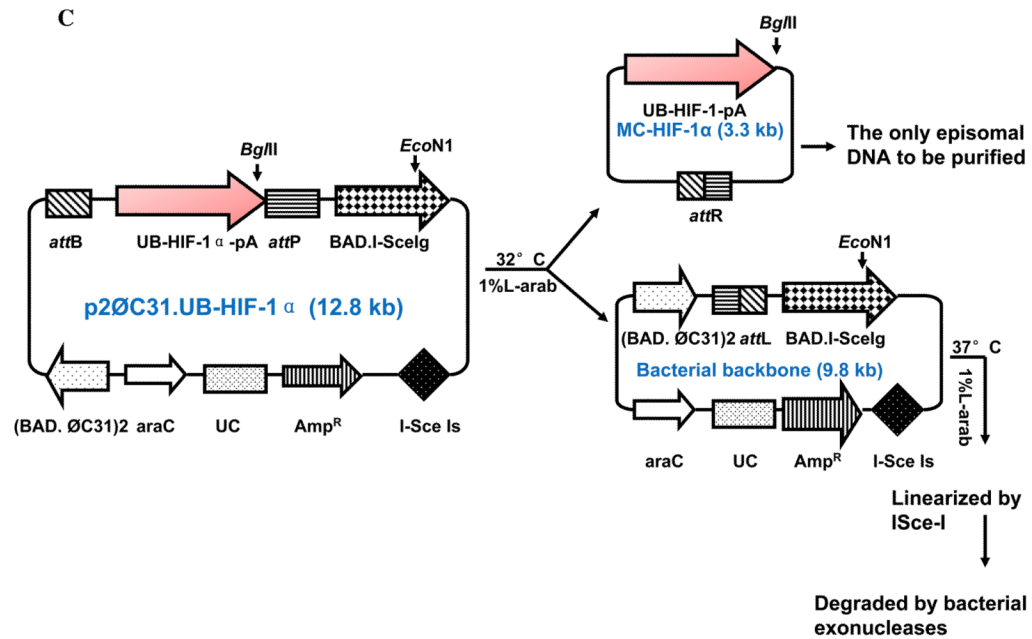


Figure 1. Schema of the non-viral minicircle plasmid

(A) Minicircles are the product of site-specific recombination between the *attB* and *attP* sites driven by bacteriophage ØC31 integrase. (B) Schema of the production process for minicircles carrying Fluc-eGFP double fusion reporter gene. By adding 1% L-arabinose to the bacterial culture media, the *att* sites of p2ØC31.UB-DF were recombined to generate the minicircle DNA. The remaining circular bacterial backbone plasmids were linearized by *I-SceI* homing endonuclease and were removed by bacterial exonucleases at 37°C. (C) Schema of the production process for minicircles carrying HIF-1α therapeutic gene. In all three schemas, the end result is two circular DNAs: one is the minicircle (MC), which contains the therapeutic gene cassette and the right hybrid sequence (*attR*), and the other is the bacterial backbone, which contains the origin of replication, the antibiotic marker, and the left hybrid sequence (*attL*).

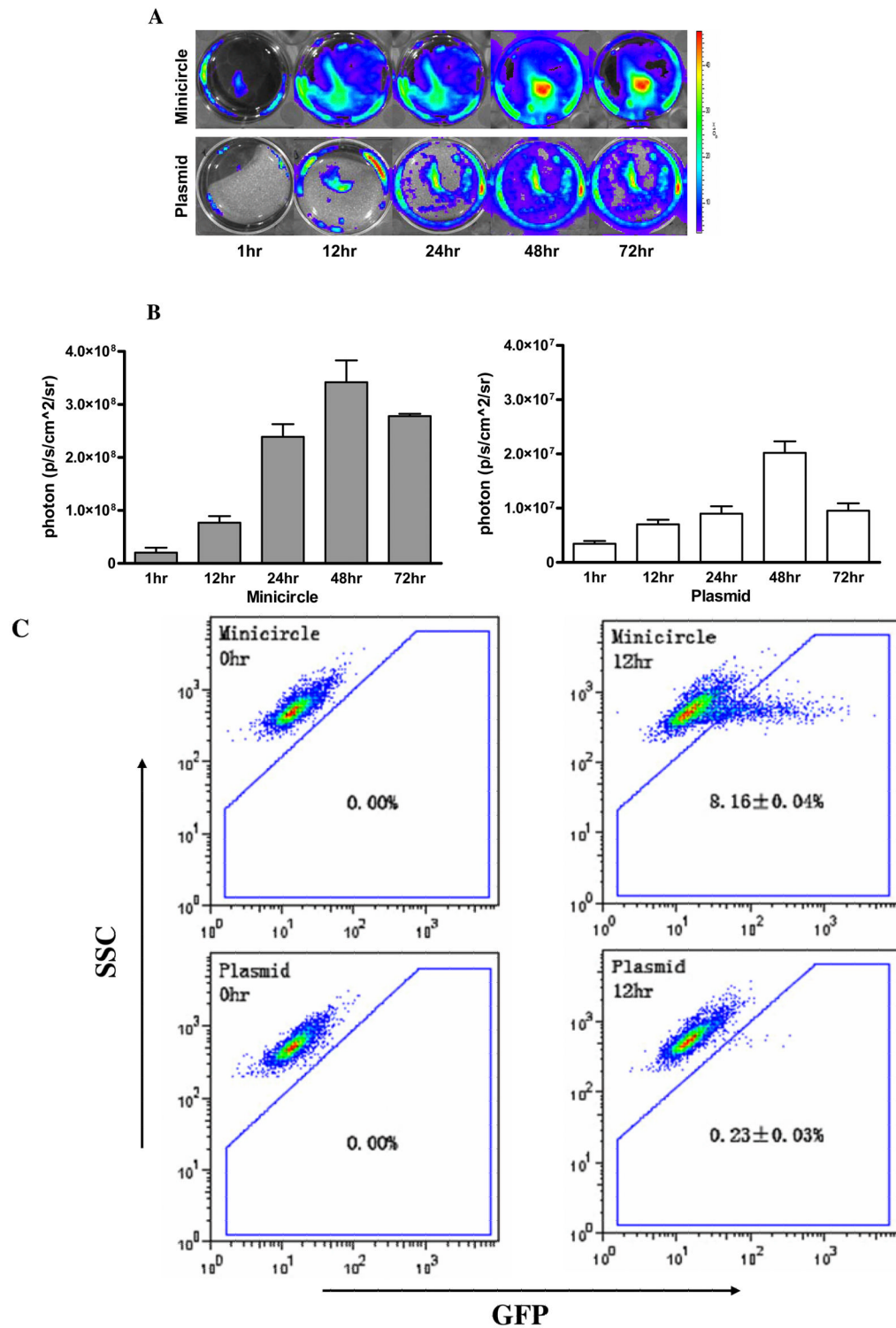


Figure 2. Comparison of minicircles vs. regular plasmids *in vitro*. (A) The DF consists of Fluc and eGFP linked by a 5-amino acid linker (GSHGD). *In vitro* BLI shows that Fluc signals are significantly higher in C2C12 cells transfected with minicircles compared to plasmids at all time points. (B) Quantitation of Fluc indicates that minicircles are 5.5±1.7 (at 12 hr) and 8.1±2.8-fold (at 48 hr) higher than regular plasmid.

Note the difference in Y-axis bars between the two plots. (C) eGFP expression through FACS at 12 hr coincides with the bioluminescence imaging results.

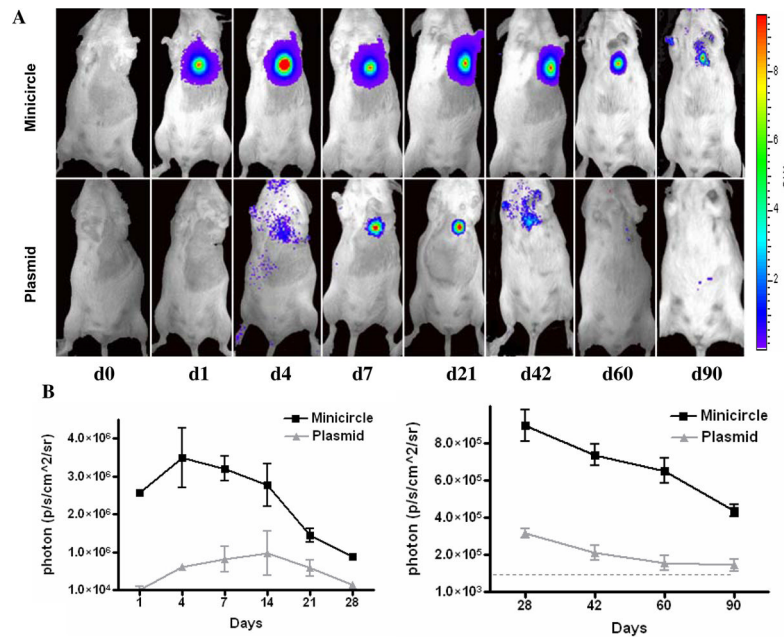


Figure 3. Comparison of minicircles vs. regular plasmids *in vivo*.

(A) Both MC-DF and PL-DF were injected into normal murine hearts. Mice injected with minicircles (top row) showed more robust Fluc signals compared to mice injected with regular plasmid (bottom row). Transgene expression was detectable at day 1, peaked at week 1–2, and lasted for >90 days. (B) Detailed quantitative analysis of Fluc bioluminescence signals from days 1–28 (left) and days 28–90 (right). Note the difference in Y-axis scale bars (as p/sec/cm²/sr) between the two plots. Background bioluminescence signal is denoted by the dashed line (1.33×10^4 p/sec/cm²/sr).

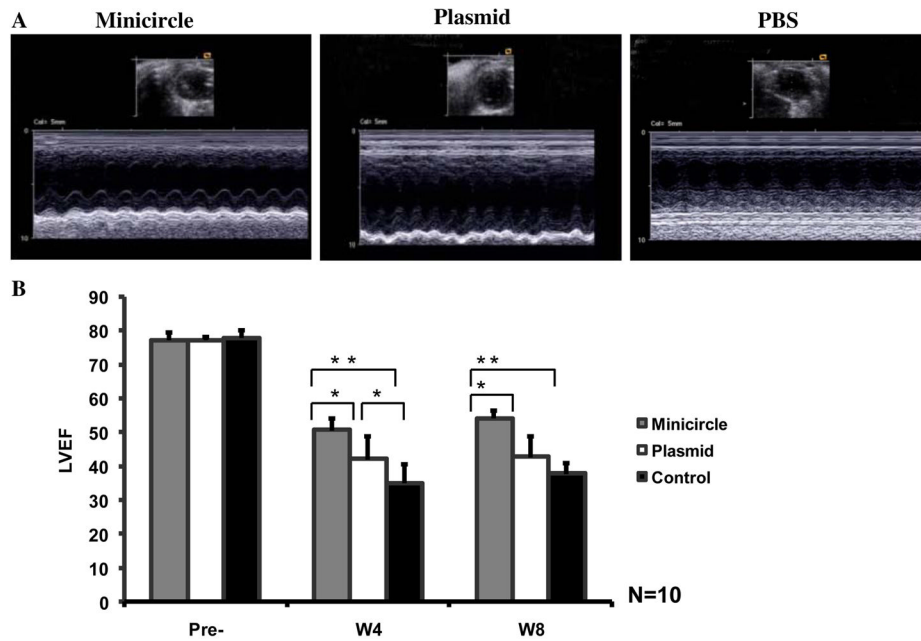


Figure 4. Evaluation of cardiac function following minicircle vs. plasmid mediated HIF-1 α therapy

(A) Representative echocardiogram (M-mode) of mice with LAD ligation following injection of minicircles (left), regular plasmid (middle), or PBS (right) as control group at week 8. (B) Quantitative analysis of left ventricular ejection fraction (LVEF) among the three groups. Compared to saline injection, animals injected with MC-HIF-1 α had significant improvements in LVEF at week 4 and week 8. Animals injected with regular plasmids had significant improvement in LVEF at week 4 but not by week 8.

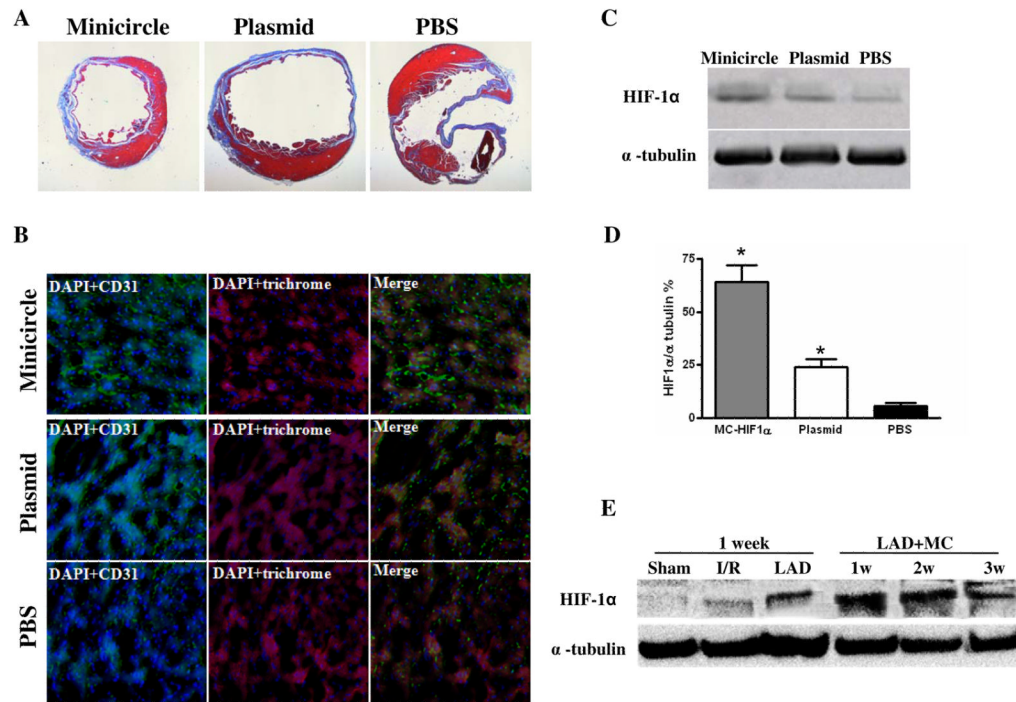


Figure 5. Confirmation of HIF-1 α overexpression in postmortem explanted hearts

(A) Representative H&E staining shows preservation of thicker heart wall mass after MC-HIF-1 α treatment compared to PL-HIF-1 α or PBS injections at week 8. (B) Immunofluorescence staining of CD31 endothelial marker (green) indicates increased small vessels in the myocardium following MC-HIF-1 α and PL-HIF-1 α therapy compared to PBS control. Cardiomyocyte staining is identified by trichrome (red; 100x magnification). Nuclear staining is identified by DAPI (blue; 100x magnification). (C-D) Representative Western blots and quantitative densitometric analysis of explanted hearts injected with MC-HIF-1 α , PL-HIF-1 α or PBS control at day 14. Significant upregulation of HIF-1 α can be seen in the minicircle group. (E) Western blot shows higher activation of endogenous HIF-1 α by LAD ligation compared to ischemia-reperfusion. Following delivery of MC-based gene therapy, HIF-1 α levels are most robust at week 1 and decreases subsequently, coinciding with similar pattern of Fluc imaging signal decay seen in Figure 3A. Sham: open thoracotomy only; I/R, ischemia/reperfusion; LAD: LAD ligation.

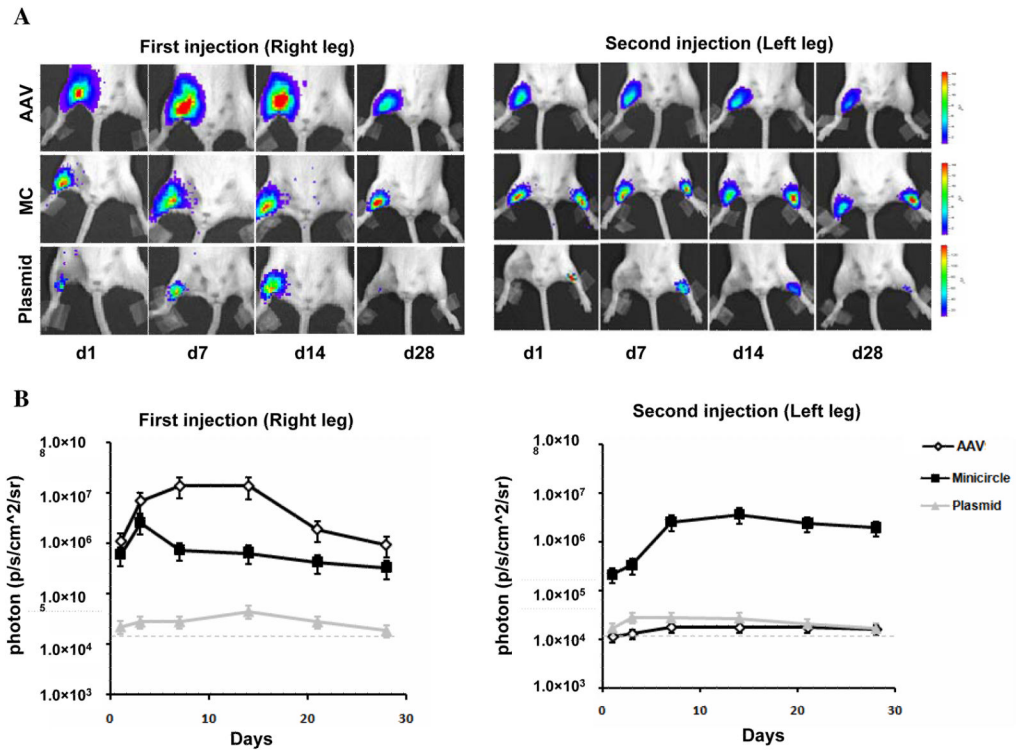


Figure 6. Comparison of viral vs. non-viral mediated gene expression

(A) Representative BLI images of animals injected with AAV, minicircle, and regular plasmid in the right leg (first injection) followed by the left leg 28 days later (second injection). As expected, AAV expression is more robust compared to MC and plasmids initially. However, following repeat injection, AAV expression is not detected in the contralateral leg due to host mediated humoral immune response. Color scale bar values are expressed as photons per second per square centimeter per steradian (p/s/cm²/sr). (B) Graphical representation of longitudinal BLI after first and second injections in all three groups. Note that day 28 of second injection in left leg would represent day 56 of first injection in right leg in the same animal.